

4.2. RADIOGRAPHIC ANATOMY OF THE LIMBS OF THE JUVENILE AND SUBADULT LOGGERHEAD SEA TURTLES (*CARETTA CARETTA*)



Valente, A.L.; Marco, I; Zamora, M.A.; Parga, M.L.; Lavín, S.; Alegre, F. y Cuenca, R. (2007). Radiographic anatomy of the limbs of the juvenile and subadult loggerhead sea turtles (*Caretta caretta*). Can. J. Vet. Res. Aceptado para publicación.

RADIOGRAPHIC ANATOMY OF THE LIMBS OF THE JUVENILE AND SUBADULT LOGGERHEAD SEA TURTLES (*Caretta caretta*).

A. L. Valente, I. Marco, M. Zamora, M. L. Parga, S. Lavin, Alegre F. and
R. Cuenca

Address of authors:

Servei d'Ecopatologia de Fauna Salvatge. Facultat de Veterinària, Universitat Autònoma de Barcelona; 08193-Bellaterra, Barcelona, Spain (Valente, Cuenca, Lavin, Marco).

Diagnosis Mèdica, Córcega, 345, Barcelona, Spain (Zamora)

Centre de Recuperació d'Animals Marins; Camí Ral 239, 08330 - Premià de Mar, Barcelona, Spain (Parga, Alegre)

Corresponding author: Ana Luisa Valente.

Servei d'Ecopatologia de Fauna Salvatge, Facultat de Veterinària, Universitat Autònoma de Barcelona; 08193-Bellaterra, Barcelona, Spain.

Telephone number: +34 93 581 19 23;

Fax number: +34 93 581 20 06;

Abstract

This study aims to provide the normal radiographic anatomy of the limbs of the loggerhead sea turtle (*Caretta caretta*). Dorso-palmar (-plantar) radiographs were taken on the fore- and hindlimbs of 15 juvenile and 15 sub-adult loggerhead sea turtles, 17 alive and 13 deceased. Additionally, computed tomography (CT), gross anatomy, osteological and histological studies were performed on the limbs of 5 of them for comparison with radiological findings. Bones from the distal part of the fore- and hind flippers were seen in detail using mammography film-screen combination. Pectoral and pelvic girdles, superimposed by the carapace, were better seen on the standard radiographs using rare-earth intensifying screens. Mammographic radiographs of the manus of 5 small juvenile turtles showed active growth zones. Visualization of bone contours on the distal part of the limbs was clearer compared with mammals due to the very few superimpositions between them. The presence of a significant cartilage in the epiphyses produced better visibility of limb-ends. We have concluded that the use of mammographic film-screen combination is the best mode to evaluate the bony and joint structures of the fore- and hindlimbs of juvenile and subadult sea turtles. Radiographs provided reliable images for clinical purposes. Considering the low cost and logistics of this technique it is one of the more practical ancillary tests that marine animal rehabilitation centres can use.

Keywords: radiographic anatomy, loggerhead sea turtle, *Caretta caretta*, limbs, diagnostic imaging.

Introduction

Sea turtle populations have declined over the past few decades due to human activity. Boat-strike injuries, entanglement in fishing nets, the swallowing of hooks, fishing lines and crude oil are the main causes of sea turtle mortality around the Canary Islands and in the Western Mediterranean (1, 2). The loggerhead sea turtle (*Caretta caretta*) is listed as endangered (3) and is the most common species accidentally caught by fishing activities in the Mediterranean Sea. Juveniles and subadults are most commonly caught and most animals rescued from fishing nets have some degree of limb trauma which occurs when turtles become entrapped in nets, leading to strangulation of extremities (2). Once at the rehabilitation centre, proper physical assessment should be performed as should a minimum standard database including blood analysis and radiographs (4).

Different imaging methods are available today for veterinary practice. However, normal radiological parameters are scarce for most free-ranging animals, including sea turtles. Previous authors have reported radiological techniques applied to reptile species (5, 6, 7, 8, 9, 10). However, due to the wide morphologic variety of reptiles, further knowledge of the normal radiographic anatomy in a particular species is required.

This article forms part of a wide-ranging study on diagnostic imaging of the loggerhead sea turtle, its purpose being to provide the normal radiographic anatomy of the limbs of the loggerhead sea turtle. We have combined radiological information with computed tomography, osteological, gross anatomical and histological data of the appendicular skeleton of this species in order to provide useful information for increasing relevant clinical knowledge.

Materials and Methods

Dorso-palmar (-plantar) radiographs were taken on the fore- and hindlimbs of 15 juvenile and 15 sub-adult loggerhead sea turtles accidentally caught in pelagic longline sets and fishing nets along the North-Western Mediterranean coast. Juvenile turtles were considered to be those with a minimum straight carapace length (SCL_{min}) of 21 to 40 cm, and sub-adults those with a SCL_{min} of 41 to 65 cm (11). Seventeen of the animals were alive and thirteen deceased. Live turtles were temporarily housed in the rehabilitation facilities of the Rescue Centre for Marine Animals (CRAM) (Premiá de Mar, Barcelona, Spain). Only turtles free of limb damage or skeleton pathology were considered for this study. The turtles were manually restrained in ventral recumbency, the limbs maintained with cellotape in a physiological position. No sedation was required; only the eyes were masked. Table-top images were taken using a Toshiba – Rotanode™ (Model E7239) x-ray tube at a 68-cm film-focal distance. Radiographs were taken using UM- MA hc, 24x30 cm for mammography medical x-ray film, a Fuji AD-MA screen (UM MAMMO fine, Fuji Photo Film Co., Ltd.; Tokyo 106-8620) and Super HR-GB, 30x40 cm film and rare-earth intensifying screens, (Fuji ECD). Using a negatoscope the radiographs were photographed and digitalized at a minimum resolution of 300dpi. Radiographs were evaluated and radiographic anatomy described when found to be consistent.

Multi-detector Computed Tomography (MDCT) of the whole body was performed in four juvenile and one subadult loggerhead sea turtles. Turtles were anaesthetized with the association of intravenous ketamine (15mg/K, Imlagene® 1000, Merial) and diazepam (0,5mg/Kg, Diazepam, Almirall Proderfarma, Prodes), injected into the dorsal cervical sinus to prevent flipper movement. Cardiac frequency was verified using a mini-doppler and the animals were carefully kept wet prior to the scan. MDCT studies were obtained by a sixteen-detector row CT scanner (Aquilion 16, Toshiba Medical, Tokyo, Japan) using the following parameters: 120 kVp, 250mA, 16 x 1mm detector configuration and a 512 x 512 matrix. The field of view ranged from 35cm to 52cm and total time examination took between 10-15 seconds, depending on the size of the turtle. The volumetric data of the limbs were reconstructed with a 1mm slice width and reconstruction interval of 0.8 mm. Three-dimension images were generated on a Vitrea computer workstation (Vitrea® version 3.0.1., Vital Images, Plymouth, MN).

In order to obtain anatomical information of the limbs from the dead turtles, five of them (2 juvenile and 3 subadult) were frozen at -80° C, and serial parallel sections from 18 to 20 mm thick were taken in the dorsal plane using an electric bone saw. The limb bones and associated joints were evaluated and samples of epiphyses of the humerus, radius, ulna, femur, tibia, fibula, metacarpal and metatarsal bones and phalanges were collected and fixed in neutral-buffered 10% formalin solution for histological study.

Five loggerhead sea turtle skeletons from the Museo de Zoología de Barcelona and the Departamento de Sanidad y Anatomía, Facultad de Veterinaria of UAB were photographed and radiographed for osteological data.

Radiologically visible structures were compared with those observed on osteological preparations, 3D CT reconstructions, gross anatomical sections and histological samples. All radiographic images were analyzed with Adobe Photoshop® (Adobe Photoshop® v 5.5, Adobe Systems Incorporated; USA) and normal and inverted (negative) images were compared.

The anatomical terminology used in this study is that of the *Nomina Anatomica Veterinaria*. In addition, specific terminology for sea turtles (12) was also applied.

Results

Bones from the distal part of the fore and hind flippers were seen in detail in radiographs using the mammography film-screen. CT reconstructions images showed best definition to examine the cortical bone, density of the matrix and trabeculas. The pectoral and pelvic girdles were better seen in the standard table-top radiographs using rare-earth intensifying screens than the mammographic film-screen combination. These regions will be not described here since they were included in a previous publication on the coelomic cavity (13). Bones from juvenile and subadult loggerhead sea turtles did not differ in form or structure; however some bony features such as the head and greater tuberosity of the humerus and the head and major trochanter of the femur were more pronounced in the subadults.

Radiographically, a large joint space was seen in all synovial joints of the limbs (Fig.1A). In the anatomical sections a thick hyaline cartilage cone plugged each bone forming the great part of the epiphyseal area (Fig. 1B). Mammographic radiographs of 5 small juvenile turtles showed a thin radiolucent line followed by a radiodense longitudinally striated and thicker band (Fig. 2A) mainly in the physes of the metacarpals, metatarsals, phalanges and distal physes of the humerus. Subcondral growth was observed in all bones. These findings were interpreted based on the histological analyses of the same animals, as active growth zones in the epiphyseal plate (Fig. 2D). Long bones consisted primarily of a core of cancellous bone bounded by a thin cortex of compact bone (Fig. 2 B-C). The histological study carried out in 2 juveniles showed that the epiphysis consisted of a mass of undifferentiated cartilage where the cells (condrocytes) of the layer next to the shaft forming the growth zone were flattened and arranged in longitudinal columns, showing different degrees of hypertrophy. Condrocytes nearest to the shaft were more vacuolated than those nearest the end of the epiphyses. In the 3 subadult turtles, the cellular arrangement in the growth area was similar to that observed in the 2 juvenile ones; however the longitudinal columns were not so well-defined. In all cases, mineralization of a cartilage template was observed and endochondral bone was set down on the eroded surface of the cartilage (Fig. 2D).

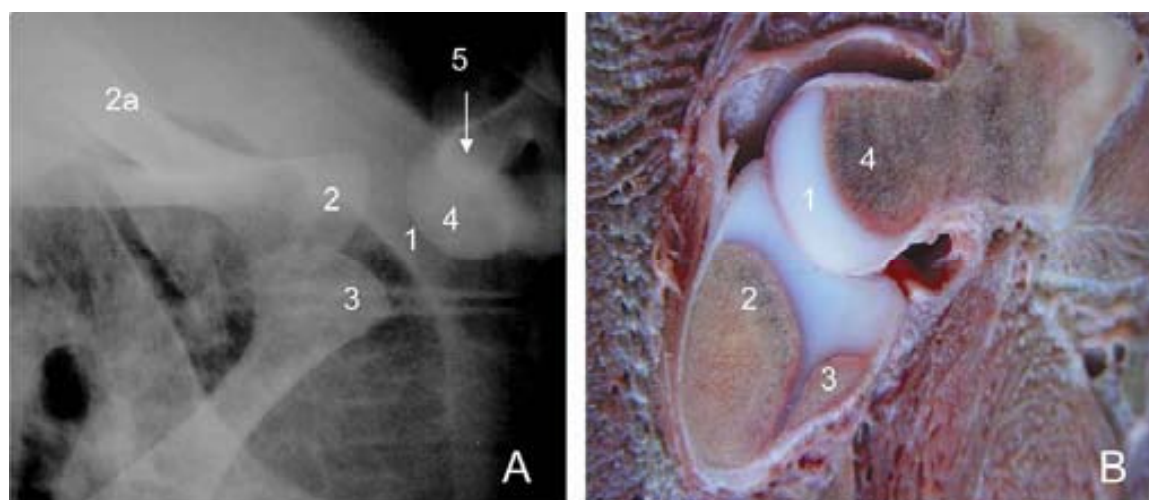


Figure 1. Dorsoventral radiographic view (A) and dorsal anatomical section (B) of the shoulder joint of a loggerhead sea turtle. 1, Cartilaginous part of humerus head. 2, articular end of the Scapula (cranial fused bone is the Acromion process – 2a); 3, articular end of the coracoid; 4, humerus head; 5, greater tuberosity.

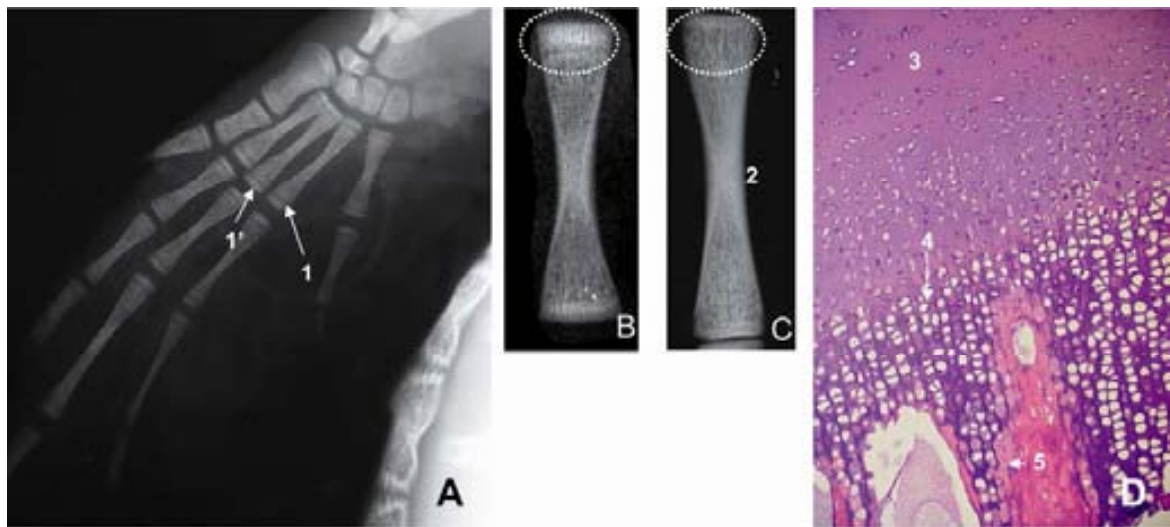


Figure 2. Dorsoventral radiographic view (A) of the manus of small juvenile loggerhead sea turtle. Close-up of proximal phalange of digit II of juvenile (B) and subadult (C) specimens. Histological survey of the growth area (C). 1, epiphyseal growth zone (1' epiphyseal plate); 2, ossified diaphysis; 3, undifferentiated cartilage; 4, longitudinal columns of hypertrophied condrocytes; 5, Mineralization of cartilage template, endochondral bone.

Humerus

The proximal epiphysis of the humerus was not clearly seen radiographically due to the superimposition of the carapace and plastron bones. The head of the bone was seen joined with the articular surface formed by the scapula and acromion and coracoid bones (Figs. 1A-B, 3A). Caudal to the head, the great and rounded medial process (greater tuberosity) was easily identified in all radiographs (Fig. 3A-C). The morphology of this structure in the radiographs was similar to the head of the humerus in both juvenile and subadult turtles (Fig. 3A, B).

However, in CT, osteological and anatomical dissections, this structure was more prominent than the head (Fig. 3C). A large fosa could be clearly seen in the radiographs as a radiolucent area immediately below the head and the greater tuberosity. The deltoid crest could be identified as a rounded projection of the bone contour on the cranial border of the humerus (Fig. 3A-C). In 3 subadult turtles, this crest was more prominent than in juveniles and, depending on the rotation of the limb at the moment of the examination, the structure was seen partially superimposed on the humeral head (Fig. 1A). In one juvenile turtle a sharp process was seen in the caudal border of the crest (Fig. 3B). The nutrient foramen present on the ventral surface of the humerus (Fig. 3C) could not be observed on all radiographs. In the distal epiphysis of the humerus, the medial and lateral condyles were recognisable due to the presence of the intertuberal groove between them (Fig. 3C, E).

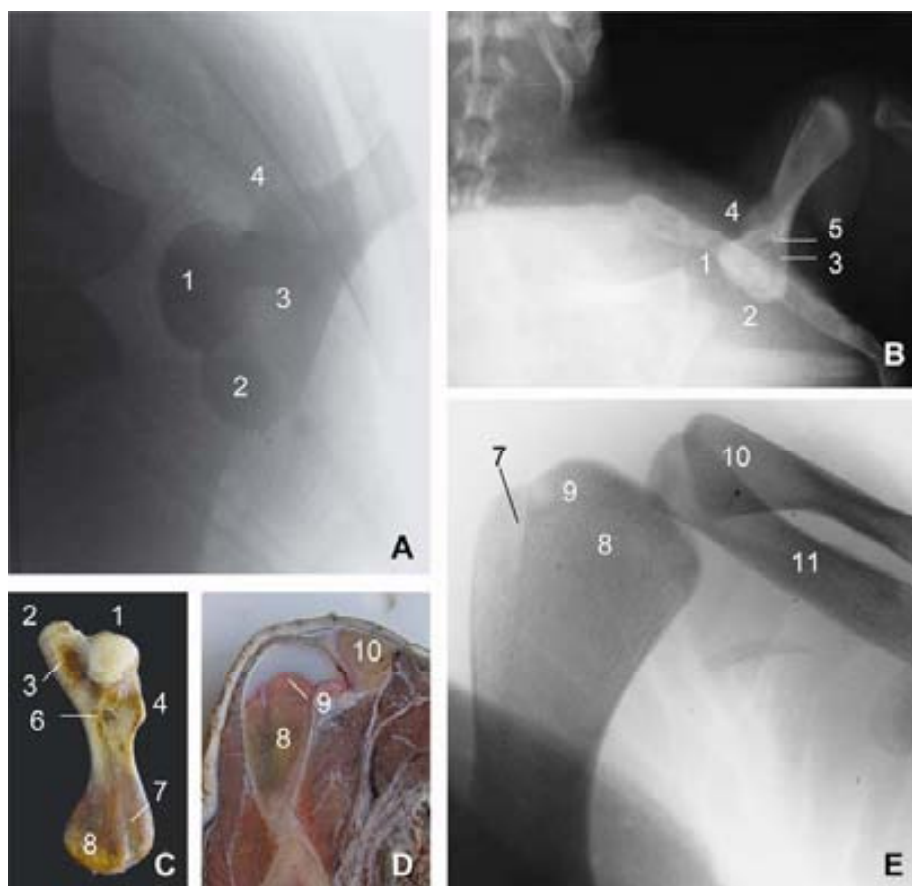


Figure 3. Negative image of dorsoventral radiographic view of humerus of sub-adult (A, E) and juvenile (B) loggerhead sea turtles; ventral view of humerus (C) and anatomical section of elbow joint (D). 1, humerus head; 2, greater tuberosity; 3, fossa between humerus head and greater tuberosity; 4, deltoid crest; 5, sharp process on deltoid crest; 6, nutrient foramen; 7, intercondylar sulcus; 8, medial condyle; 9, growth zone; 10, radius; 11, ulna.

Radius and ulna

The bones were seen partially superimposed, the radius, shorter than the ulna was seen cranial to it. The radius had a broad and triangular proximal epiphysis and its caudal border showed a concave curvature. The ulna was seen as straight and tubular shaped with its distal end superimposed on the ulnare and radiale carpal bones (Fig. 3E, 4A). No pronounced process or grooves were visualized in either bones and the cortices were markedly thickened in the mid-diaphyseal region but tapered proximally and distally (Figs. 3E, 4A).

Carpal bones

The nine carpal bones could be clearly recognized in the carpus due to scant superimposition (Fig. 4A-C). In the proximal row, the radiale was seen as a rectangular bone placed laterally. The ulnare showed a semilunar shape,

with a great curvature pointed medially. The pisiform bone was seen standing out medially from the distal row. The small and rounded centrale bone was seen immediately ventral to the radiale and ulnare bones. In the distal row of the carpus, five carpal bones were identified, each one respective to a digit (Fig. 4C).

Metacarpals and phalanges

Metacarpals bones and phalanges have similarly-shaped digits except for the first, which shows a flattened articular surface on the physes and elongated, thin diaphyses. The first digit is prominent and consists of a short and strong metacarpal bone with only two sturdy phalanges, the proximal and distal ones (Fig 4A). The second digit has a shorter and thicker proximal phalange than those of the 3rd and 4th digits. The intermediate phalange of the third digit is the most slender and longest of all. The fifth digit has only two phalanges. In the radiographs and CT images, no sesamoid bones were seen associated with the flipper joints (Fig. 4 A, B).

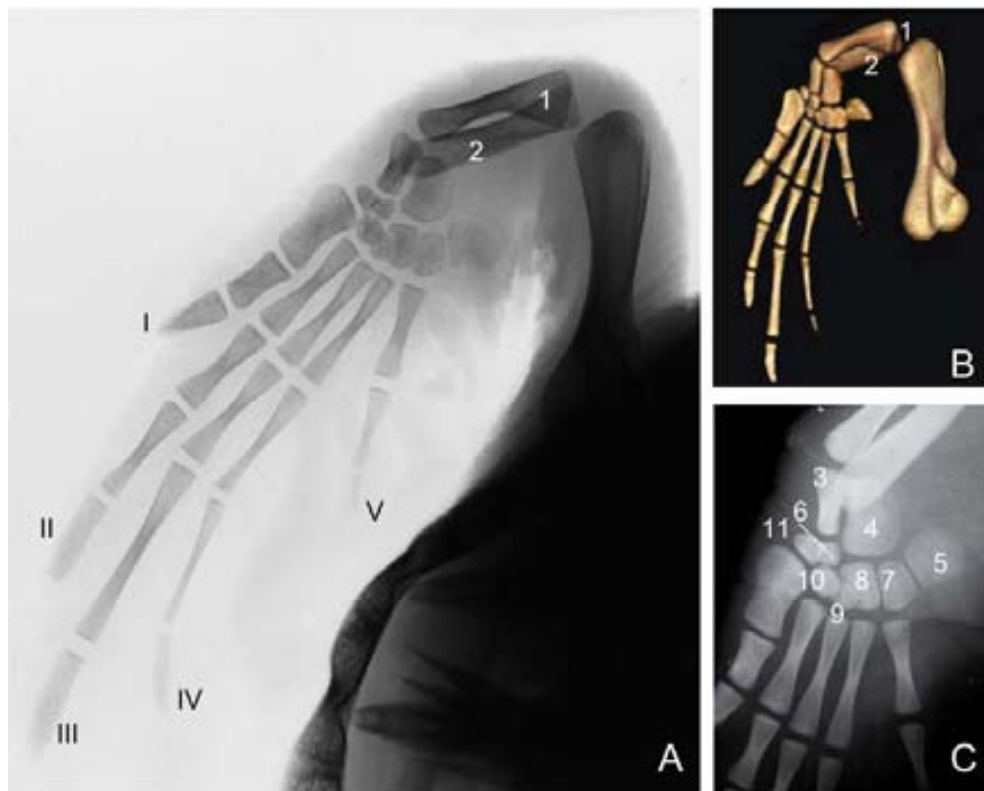


Figure 4. Negative image of dorsoventral radiographic view (A) and 3-D reconstruction (B) of *manus* of juvenile loggerhead sea turtle. Close-up of dorsoventral radiographic view of carpal region (C). 1, radius; 2, ulna; 3, radiale; 4, ulnare; 5, pisiform; 6, centrale bone; 7,8,9,10,11, carpal bones. Roman numbers in A indicate respective digit.

Femur

The joint of the head of the femur with the acetabulum superimposed on the carapace bones was clearly visible in all radiographs taken using conventional plain film (Fig. 5A, B). In juvenile turtles, most of the head was made up of cartilage. In the subadult animals the ossified head was stouter than in juvenile and was joined to the physes through a thick neck (Fig 5A-E). The prominent major trochanter was seen caudal to the head. The diaphysis was long and slender. The condyles on the distal epiphyses could not be differentiated because the distal epiphysis was superimposed on the marginal bones of the carapace. Neither the patella nor other sesamoid bones were visualized in the stifle joint (Fig. 5A, 6B).

Tibia and fibula

The tibia and fibula could be seen with scant superimposition of epiphyses. The tibia was thicker, cranial to the fibula, and with a convex articular surface at the proximal epiphysis. Both bones were elongated and fairly similar in length (Fig. 6A, B).

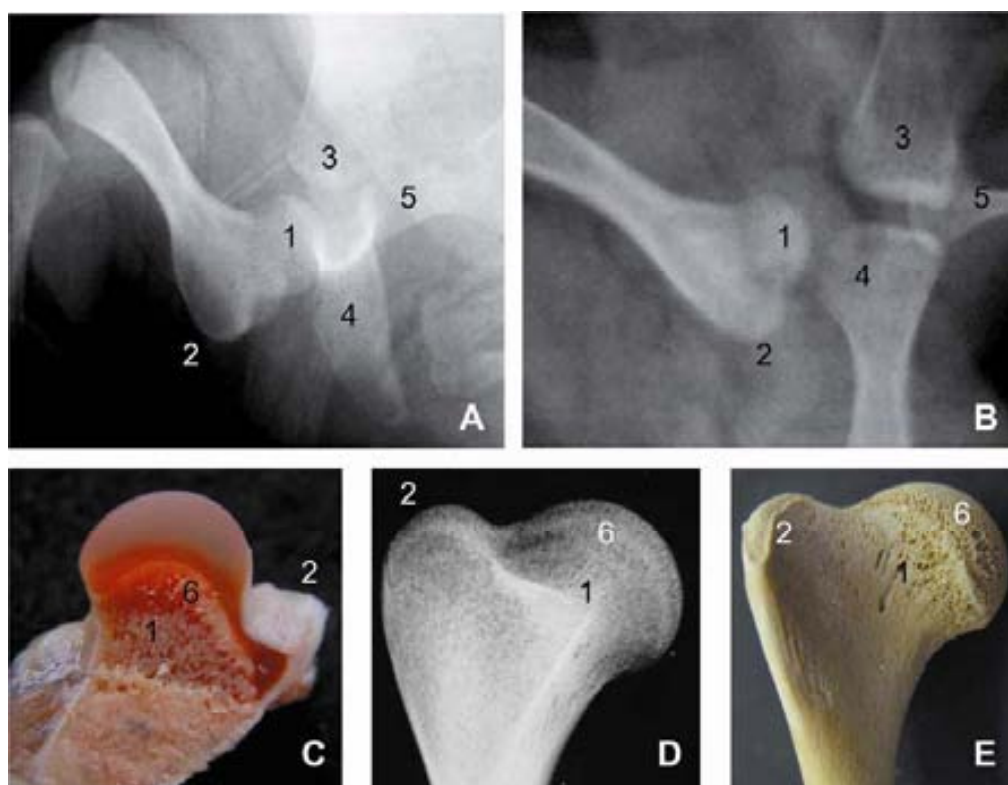


Figure 5. Dorsoventral radiographic view of hip joint of sub-adult (A) and juvenile (B) loggerhead sea turtles. Gross anatomy section (C), radiographic view (D) and osteological preparation (E) of proximal epiphysis of femur. 1, femoral head; 2, greater trochanter; 3, pubis; 4, ilium; 5, ischium; 6, growth zone.

Tarsal bones

Six tarsal bones were perfectly visualized in all radiographs. We have identified two rounded and bigger ones and four quite spherical and smaller ones (Fig. 6 A-C). On the proximal row the great astragalus was seen laterally below the tibia, and the calcaneum seen as a small rounded bone positioned medially below the fibula (Fig.6C). In the distal row, the V tarsal bone was articulated with the IV and V metatarsal bones and was prominent because of its heart shape and the large size related to other tarsal bones, which were spherical and positioned just proximal to each respective digit, I, II and III (Fig. 6C).

Metatarsals and phalanges

Similar to the forelimb, the first digit consisted of a short, flattened and strong metatarsal bone and only two sturdy phalanges. Digits II to V showed three somewhat proportioned phalanges. The V metatarsal bone is flattened and resembles the I metatarsal bone, though slightly smaller (Fig.6 A, B).

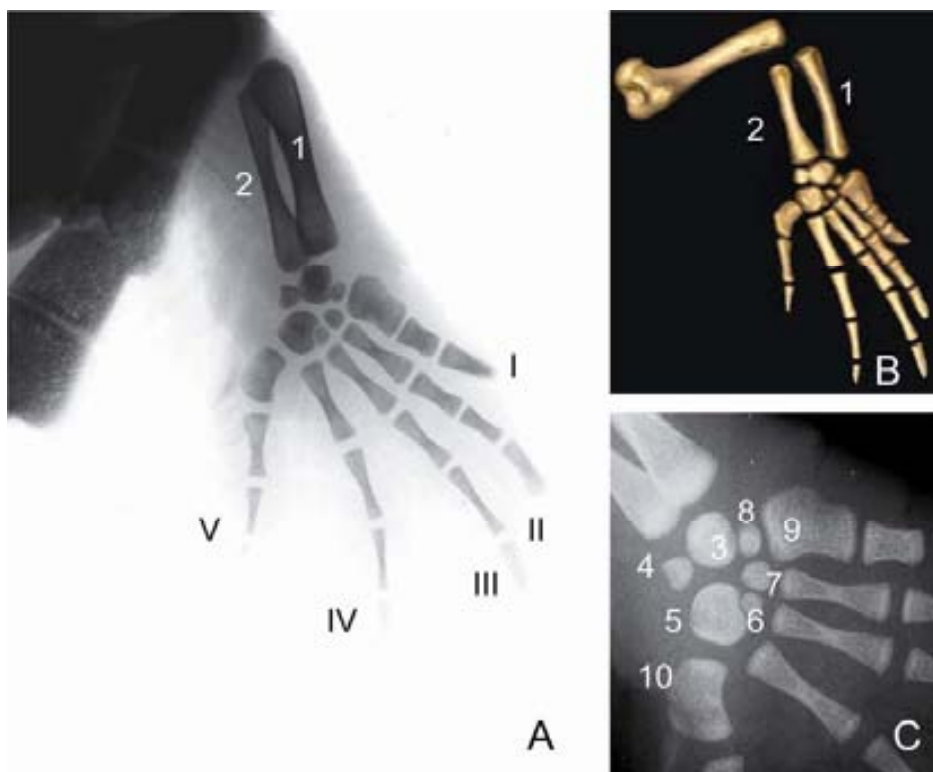


Figure 6. Negative image of dorsoventral radiographic view (A) and 3-D reconstruction (B) of *pedis* of juvenile loggerhead sea turtle. Close-up of dorsoventral radiographic view of tarsal region (C). 1, tibia; 2, fibula; 3, astragalus; 4, calcaneum; 5, V tarsal bone; 6, 7, 8, tarsal bones; 9, metatarsal bone from digit I; 10, metatarsal bone from digit V. Roman numbers in A indicate respective digit.

Discussion

Routine radiography of the limbs is usually performed in at least three views: dorso-palmar (or -plantar), lateral and oblique (14). The flattened shape and relative thinness of the loggerhead sea turtles' flippers when compared with the compact and quite cylindrical limbs of the terrestrial vertebrates precludes the use of other views except the dorso-palmar (-plantar). Size or morphological distortion was observed only at the proximal end of the humerus, where the great tuberosity was seen partially superimposed on itself showing an unreal shape in the radiographs. Numerous anatomical differences between the limbs of chelonians and those of mammals, or even between turtles and other reptiles, make them a unique patient. When comparing radiographs of limbs of sea turtles with those of mammals, such as the dog or cat, there is a clearer visualization of the bone contours due to the scant superimpositions between them. Additionally, the presence of a massive cartilage in the epiphyses produced better visibility of the articular ends. According to previous information (15) these cartilaginous epiphyses become gradually thinner with age because the passage of undifferentiated cells into the growth zone and consequently the articular and growth zones come into close approximation; however growth may be retained even in aged animals. Easy visualization of the bone ends was a finding with practical clinical application because the diagnosis of bone disorders such as fractures, osteomyelitis, osteofibrosis and mainly joint pathologies could be easily made using a conventional and inexpensive x-ray technique.

Previous studies (8) have reported that the matched mammography film-screen combination was superior to standard Buchy and table-top radiographs in the evaluation of bone and soft tissues in small reptiles. The combination results in a resolution of 10-20 line pairs (lp)/mm as opposed to the 5-10 lp/mm resolution in standard radiographic techniques (8), which in this study permitted optimal visualization of the cancellous and compact bone arrangement in the long bones, and the epiphyseal growth areas. The growth areas observed in our animals as a radiopaque band at the end of the long bones were also observed in skeletally immature humans (16), where transverse trabecular bands of increased radiodensity appeared following a temporary slowdown or cessation of rapid longitudinal bone formation. When growth rates were normal, longitudinally-oriented trabeculae with interspersed marrow elements predominated at the zone of transformation of cartilage to bone (16).

Radiological examination of the long bone epiphyses together with evaluation of time of closure have been used as a chronological reference in various species of vertebrates (17, 18). In reptiles this methodology is not suitable because endochondral growth may be life-long (15). On the other hand, turtles and crocodiles do not have isolated ossification centres in the epiphysis (bony epiphysis) such as occurs with squamates (snakes and lizards) and mammals (15). Curiously, in our study only in 5 of 15 juvenile turtles was the presence of epiphyseal plates detected radiographically in the long bones of the manus. We are unaware of the reasons why these areas were not seen in all juvenile animals, as should be expected. Patterns of reptile growth have attracted considerable attention over the past few decades (19, 20, 21). The presence of growth rings in the transverse section of the humerus has been studied in reptiles, including sea turtles (22), as a method to calculate age. Turtles grow at different rates during the ontogenetic period, the rate being influenced quality and quantity of diet (15, 23). In their early years of life, oceanic-stage loggerhead

sea turtles have relatively little control over their geographic position or movements and thus they have an extremely stochastic lifestyle with great variation in food availability and temperature (24). Temporary cessation of growth may occur even in relatively young turtles; it is resumed later, after perforation of the bony plates and renewal of activity by the marrow (15). The environmental variation results in variable growth rates, that could be directly associated with the inconsistent presence of a distinct growth area in the long bones of juvenile turtles of this study.

The shape and structure of bones is governed by many factors - genetic, metabolic and mechanical. In reptiles, the pectoral and pelvic arches appear to have a very anomalous position in the Chelonia, inasmuch as they seem to be situated inside and not outside the skeleton trunk (12). Modifications of the sea turtle pectoral limb into a semi-rigid elongated and flattened flipper for forelimb propulsion has resulted in proportional changes in the limb skeleton and shifts in the distributions of muscle tissue (25). This reduced presence of musculoskeletal elements includes the sesamoid bones, thus accounting for their absence in the radiographs of the present study. Although reptilian compact bone is quite similar to the other vertebrates, we have found the bone cortex to be relatively thinner in the case of turtles, with minor radiographic contrast between bones. Compared to the radiographic anatomy of well-known species such as the dog or cat (26), the diaphysis of turtle bones in general seems to show a smoother surface without pronounced processes, crests or tuberosities. As a result, there is a clearer radiographical image of the bone internal structure, with minimal superimposition of superficial bony elements. The response pattern of the bone to injury in reptiles differs significantly from that found in mammals. New periosteal bone production is less prominent in the former and it is common to see a radiolucent fracture line in clinically stable fractures that have healed with a fibrous callus (10, 27).

Mammographic radiographs and the multiplanar TC reconstructions were observed to provide similar information; the latter also involved greater cost and is a technique not readily available in rehabilitation centers. Also, more time is needed for image manipulation. Three-dimension reconstructions were useful to see the different views of the structures. However, this kind of virtual processing, when applied to extremely tight bone structures, as is the case with carpal or tarsal bones, may produce an artificial effect whereby the structures seems to be joined.

In this study we have concluded that the use of mammographic film-screen combination is the best radiographic modality to evaluate the bone and joint structures of the fore and hindlimbs of juvenile and subadult sea turtles. Radiographs provided reliable images for clinical purposes. Considering the low cost and logistics of this technique it is one of the more practical ancillary tests that marine animal rehabilitation centres can use.

Acknowledgments

The authors would like to thank Professor Dr. Francisco Reina and the laboratory technician Isabel Delgado Calvarro, Facultat de Medicina, UAB, for help with the anatomical sections, and the radio-diagnostic technician Montse March for technical support with the MDCT. Thanks also go to the Museo de Zoología de Barcelona and the Depto. de Sanidad y Anatomía, Facultat de Veterinaria of the UAB for providing the turtle skeletons. We are grateful to Dr. Jordi Franch, Depto de Medicina y Cirugia Animal, Facultat de Veterinaria of the UAB for the review of this paper.

References

1. Orós J, Torrent A, Calabuig P, Déniz S. Diseases and causes of mortality among sea turtles stranded in the Canary Islands, Spain (1998-2001). *Dis Aquat Organ* 2005;63:13-24.
2. Pont SG, Alegre FN. Work of the Foundation for the Conservation and Recovery of Marine Life. *Marine Turtle Newsletter* 2000;87:5-7.
3. IUCN. Red List of Threatened Species 2004. www.iucnredlist.org. Accessed February 22, 2006.
4. Wyneken J, Mader DR, Weber III ES, Merigo C. Medical care of sea turtles. In: Mader DR ed. *Reptile Medicine and Surgery*. Canada: Elsevier Inc., 2006:972-1007.
5. Wyneken J. Computed tomography and Magnetic resonance imaging anatomy of reptiles. In: Mader DR ed. *Reptile Medicine and Surgery*. Canada: Elsevier Inc., 2006:1088-1096.
6. Rübél A, Kuoni W. Radiology and Imaging. In: Frye FL ed. *Biomedical and surgical aspects of captive reptile husbandry*. 2nd ed. USA: Krieger Pub. Co., 1991:185-208.
7. Jackson OF, Sainsbury AW. Radiological and related investigations. In: Beynon PH, ed. *BSAVA Manual of Reptiles*. British Small Animal Association. Dorset: J. Looker Printers, 1992: 63-72.
8. DeShaw B, Schoenfeld A, Cook RA, Haramati N. Imaging of Reptiles: a comparison study of various radiographic techniques. *J Zoo Wildl Med* 1996;27: 364-370.
9. Hernandez-Divers S, Hernandez-Divers S. Diagnostic imaging of reptiles. *In Practice* 2001; july/august: 370-391.
10. Wilkinson R, Hernandez-Divers S, Lafortune M, Calvert I, Gumpenberger M, McArthur S. Diagnostic Imaging. In: McArthur S, Wilkinson R, Meyer J, eds. *Medicine and Surgery of tortoises and turtles*. Victoria, Australia: Blackell Publishing Ltd., 2004:187-238.
11. Dodd CK Jr. Synopsis of the biological data on the loggerhead sea turtle *Caretta* (Linnaeus 1758). U.S. Fish and Wildlife Service Biological Report 1988;88:35-82
12. Wyneken J. The Anatomy of Sea Turtles. U.S. Department of Commerce NOAA Technical Memorandum NMFS-SEFSC 2001;470:1-172.
13. Valente AL, Cuenca R, Parga ML, Lavin S, Franch J, Marco I. Cervical and coelomic radiology of the Loggerhead Sea turtle, *Caretta caretta*. *Can J Vet Res* (in press).
14. Morgan JP. *Techniques of veterinary radiography*. Iowa State University Press, Ames, Iowa, 1993.
15. Haines RW. Epiphyses and sesamoids. In: Gans C, d'A Bellairs A, eds. *Biology of the Reptilia*. New York: Academic Press, 1969:81-115
16. Ogden JA. Growth slowdown and arrest lines. *J. Pediatr Orthop* 1984;4:409-415.
17. DiGiancamillo M, Rattegni G, Podestà M, Cagnolaro L, Cozzi B, Leonardo L. Postnatal ossification of the thoracic limb in striped dolphins (*Stenella coeruleoalba*) (Meyen, 1833) from the Mediterranean Sea. *Can J Zool* 1998;76:1286-1293.
18. Serrano E, Gállego L, Pérez JM. Ossification of the Appendicular Skeleton in the Spanish Bies *Capra pyrenaica* Schinz, 1838 (Artiodactyla: Bovidae), with Regard to Determination of Age. *Anat Histo. Embryol* 2004;33: 33-37.
19. Hailey A, Coulson IM. The growth pattern of the African tortoise *Geochelone pardalis* and other chelonians. *Can J Zool* 1999;77:181-193.
20. Bjorndal KA, Bolten AB, Martins HR. Somatic growth model of juvenile loggerhead sea turtles *Caretta caretta*: duration of pelagic stage. *Mar Ecol Prog Ser* 2000;202:265-272.

21. Arcos-García JL, Peralta MAC, Rosales VHR, Martínez GDM, Cerrilla MEO, Sánchez FC. Growth characterization of black iguana (*Ctenosaura pectinata*) in captivity. *Vet Mex* 2002;33:409-419.
22. Zug GR, Wynn A, Ruckdeschel C. Age Estimates of Cumberland Island Loggerhead Sea Turtles. *Marine Turtle Newsletter* 1983; 25:9-11.
23. Spencer RJ. Growth patterns of two distributed freshwater turtles and a comparison of common methods used to estimate age. *Aust J Zoo* 2002;50:477-490.
24. Bjorndal KA, Bolten AB, Dellinger T, Delgado C, Martins HR. Compensatory growth in oceanic loggerhead sea turtles: response to a stochastic environment. *Ecology* 2003;84:1237-1249.
25. Wyneken J. Comparative and functional considerations of locomotion in turtles. [PhD dissertation]. Urbana-Champaign. University of Illinois, 1988.
26. Konde LJ. Appendicular Skeleton – Companion Animals. Diseases of the Immature skeleton. In: DE Thrall, ed. *Textbook of Veterinary Diagnostic Radiology*. Philadelphia: WB Saunders, 1994:94-104.
27. Silverman S. Diagnostic Imaging. In: Mader DR, ed. *Reptile Medicine and Surgery*. USA: W.B. Saunders, 2006:471-489.

